BNL-NUREG--46429

DE92 005391

ANALYSIS OF POSTULATED EVENTS FOR THE REVISED ALMR/PRISM DESIGN*

G. C. Slovik and G. J. Van Tuyle
Brookhaven National Laboratory

ABSTRACT

The Nuclear Regulatory Commission (NRC) is continuing a pre-application review of the 471 MWt, Liquid Metal Reactor, PRISM by General Electric, with Brookhaven National Laboratory providing technical support. The revised design has been evaluated, using the SSC code, for an unscrammed loss of heat sink (ULOHS), an unscrammed loss of flow (ULOF) with and without the Gas Expansion Modules (GEMs), and a 40¢ unscrammed transient overpower (UTOP) event. The feedback effects for U-27Pu-10Zr metal fuel were modeled in SSC. The ULOHS accident was determined to be a benign event for the design, with the reactor power transitioning down to a decay heat level within 500s. The power during the postulated ULOF events, with the GEMs functioning, transitioned to decay heat levels without fuel damage, and included a 300K margin to sodium saturation. The case without the GEMs had only a 160K margin to sodium saturation and higher fuel temperatures. In addition, the clad was predicted to quickly pass through the eutectic phase (between fuel and clad), and some clad wastage would result. The 40¢ UTOP was predicted to raise the power to 1.8 rated, which later stabilized near 1.2 times full power. SSC predicted some localized fuel melting for the event, but the significance of this localized damage has not yet been determined. If necessary, the vendor has options to reduce the maximum reactivity insertion below 40¢.

1. INTRODUCTION

The Nuclear Regulatory Commission (NRC), with technical support provided by the Brookhaven National Laboratory (BNL), is continuing a pre-application review of the 471 MWt PRISM advanced reactor design. The evaluation of the initial design has already been released (Ref. 1) with the supporting technical analyses performed by BNL (Ref. 2). Among the findings of the report was the determination that there were apparent vulnerabilities in the passive shutdown response to certain improbable, unscrammed, events. In particular, events which involved a rapid flow reduction without scram were of concern since the sodium margin to sodium boiling was not large enough to account for all the uncertainties. Since boiling of the sodium could introduce positive reactivity and trigger a power excursion, any potential for sodium boiling is a cause for concern.

In response to the initial findings by the NRC (Ref. 1), General Electric (G.E.) revised the PRISM design (Ref. 3). In several cases, the changes were made to directly address the NRC concerns. Other changes were dictated by the U.S. Department of Energy (DOE) as design improvements or revisions to enhance the economics of the plant. As the result of these changes, nearly all of the

*This work was performed under the auspices of the U.S. Nuclear Regulatory Commission.

DISCLAIMER

BNL analyses were repeated to factor in the new components and the revised operating conditions. Key findings with respect to the postulated unscrammed cases are summarized in this paper.

2. THE ALMR DESIGN

The ALMR plant, as presently proposed by G.E., consists of three identical power blocks of 465 MWe, for a total plant electrical rating of 1395 MWe (Table 1 and Figure 1). Each power block is comprised of three reactor modules with individual thermal ratings of 471 MWt. Each module has its own steam generator which is combined in each power block to feed a single turbine generator. The reactor module (Figure 2) is about 19 meters (62 feet) high and about 6 meters (20 feet) in diameter, and is placed in a silo (i.e., below grade).

Under normal operating conditions, four EM pumps draw sodium from the cold pool and drive it through eight pipes to the core inlet plenum. The sodium is heated as it passes upward through the fuel assemblies (hexagonal cans containing wire wrapped pins) and into the hot pool above the core region. The heat is transferred to the intermediate loop sodium by the intermediate heat exchanger (IHX), as the primary sodium passes from the hot pool to the cold pool.

The core design is illustrated in Figure 3. A "limited free bow" constraint system is utilized to assure an outward bow in the active core region of the assemblies as long as the peak temperatures are in the core center and decrease radially. The bowing is only one of several reactivity feedbacks that are significant. The other feedbacks are Doppler, sodium density, fuel expansion, core radial expansion (via grid plate and above core load pads), the control rod drive line expansion, and the Gas Expansion Modules (GEMs). Most of these feedbacks are negative for off nominal conditions, since increasing the power and core average temperature causes the core criticality to decrease. This characteristic gives the core power the tendency to transition to a lower level at an elevated temperature (unless the sodium boils). Predictive calculations are performed to determine the rate, direction, and magnitude of the reactivity feedback components during postulated transients. Linkage between the reactor modules is only through the turbine systems, and is further reduced by the use of a saturated steam cycle. As a result, one can generally decouple the reactor modules, particularly for the shorter unscrammed events.

Table 1. ALMR Plant Design Data

Reactors Modules Per Power Block:		Three
Number of Power Blocks:		One/Two/Three
Electrical Output:		465/930/1395 MWe
Reactor Power:		471 MWt
Turbine Throttle Conditions:		7.58 MPa (Saturated)
Primary Sodium	Inlet:	610K
	Outlet:	758K
Secondary Sodium	Inlet:	555K
	Outlet:	716K
Peak Fuel Pin Linear Power:		305 W/cm
Peak Fuel Burnup:		135 MWd/kg
Refueling Interval:		18 months

3. PRISM SHUTDOWN AND HEAT REMOVAL

The PRISM reactor shutdown system utilizes six control rods, with each control rod capable of shutting the reactor down. Extensive diversity in the system, i.e., each rod has its own electrical system, independent drive motors,

and a gravity drop alternative, greatly reduces the likelihood of this system failing entirely.

In the center of the core is a hollow assembly beneath a container holding B_4C balls. Dropping the balls is another independent means of terminating power. G.E. calls this system the "Ultimate Shutdown System" (USS). However this is a comparatively slow system, which requires a minute or two to respond.

When the passive-shutdown response is triggered, it can reduce the reactor power in response to most postulated unscrammed events. However, criticality of the system must be terminated as soon as possible to remove the risk of uncertainties. The potential for positive reactivity insertions through sodium boiling, or fuel relocation, dictates that this class of events be evaluated. Calculations provided the timing at which events progress and gave insight into the inherent response of the system during unscrammed events.

If there is failure to remove enough heat from the primary system, the sodium will expand, and the hot pool sodium will eventually (a few hours) spill over the reactor vessel liner. This will establish an alternate flow path and will increase the heat being rejected off the reactor vessel surface to the atmosphere (Figure 2). Once this has occurred, the Reactor Vessel Auxiliary Cooling System (RVACS) becomes fully functional and removes the decay heat load efficiently enough to prevent damage to the reactor vessel and other key components. Even without the spill-over, including normal operating conditions, there is substantial parasitic heat removal by conductance through the vessel liner, vessel, and containment vessel.

In the PRISM design, the use of sodium coolant and the relatively small reactor power facilitates this type of passive decay heat removal. Both the normal cooling and auxiliary cooling system (ACS is a natural circulation air jacket around the steam generator) can work well under natural circulation conditions. However, G.E. prefers to emphasize the RVACS performance rather than the reliability of the normal plant cooling systems. It is very difficult to completely fail this system even if partial blockages of atmospheric air are postulated. Even if all three heat removal systems fail completely, it would be at least twelve hours before significant core damage would result, because of the large thermal mass of the system.

4. U-10Zr-27PU FUEL

The current metal fuel composition proposed for PRISM is U-10Zr-27Pu. The initial data indicates that the burnup response of the ternary metal fuel is more complex than that for the original U-Zr metal fuel, showing axial expansion early in the burnup cycle, as well as fuel component migration. In theory, the behavior of the three component ternary fuel should be more complex than binary fuel, and it should require some time to characterize fully. Argonne National Laboratory (ANL) will be obtaining more data on the ternary fuel within the next year and hopes to address some of the questions that have resulted from the data obtained from the first few pins. The radial migration of the uranium and zirconium components during burnup is very substantial and causes large changes in local fuel thermal conductivities and significant changes in the fuel solidus and liquidus temperatures. In addition, there may be some radial relocation of the plutonium component, which could change the radial power distribution within the fuel pin. Consequently, some problems with metal fuel have been identified, but judgement will be reserved until more conclusive data has been compiled.

5. PRISM MODELING

The SSC (Ref. 4) and MINET (Ref. 5) codes were used in this analysis for complimentary purposes. SSC was developed at BNL for analyzing LMR transients.

SSC can model core regions in detail, as well as the primary system, the IHX, intermediate loop, steam generator, and the major components of the ternary loop. However, alternate flow patterns that may develop during loss of heat sink events or certain loss of flow can become very complicated, which requires the MINET flexibility for that part of the analysis.

5.1 SSC Model

In Figure 4 a schematic drawing of the PRISM model is shown. The core was represented using 7 channels: fuel (or driver), internal blanket, radial blanket, control assembly, shield assemblies, hot driver, and hot internal blanket. Each channel has 2 axial nodes in the lower shield, 6 axial nodes in the fuel region, and 4 nodes to represent the upper gas plenum.

5.2 Reactivity Feedback Models

Several reactivity feedbacks are important in the passive shutdown response for the metal cores. Because of the smaller Doppler feedback in the metal core, reactivity feedbacks having little importance in oxide cores are significant in the metal core. The main reactivity feedbacks are as follows:

5.2.1 Doppler Feedback

As the fuel temperature increases, more neutrons are parasitically absorbed in the resonance energy range. For metal fuel, Doppler feedback is smaller than it is for oxide fuel because of the harder neutron energy spectrum, which places fewer neutrons in the resonance energy range. Also, due to high thermal conductivity, metal fuel operating temperatures are much lower than those in oxide fuel cores. This allows the power and temperature defect in a metal core to be small (~$1.20), allowing the criticality of the system to be influenced by other natural feedbacks.

Each of the 6 axial levels in the SSC fuel representation was given equal weight and was referenced to the cold shutdown temperature. The Doppler coefficient is given in the form of:

$$\alpha = T \frac{dk}{dT},$$

which leads to the reactivity equation for the Doppler as:

$$\rho_R^{(t)} = \sum_{i=1}^{3} \sum_{j=1}^{6} \alpha_i \ln\left(\frac{T_{avj}}{T_{Ref}}\right) - \rho_{Ro}, \qquad (1)$$

k = Multiplication factor
α_i = Node Weighted Doppler Coefficient
T_{AV} = Average Node Fuel Temperature
T_{Ref} = Reference Fuel Temperature on an Absolute Scale (K or R)
j = 6 Axial Levels in the Fuel Channel
i = 3 Different Fuel Channels (i.e., driver, internal blanket, and radial blanket)

ρ_{Ro} = Steady-State Reference Value for Doppler Reactivity

The standard definition of neutronic reactivity is used (i.e., $\rho = \frac{k-1}{k}$.)

By definition, the reactivities are referenced to zero at the steady state conditions, i.e., before the transient begins.

5.2.2 Axial Fuel Expansion

Metal fuel expands axially when it heats up. Axial expansion increases the core height and decreases the effective density of the core material. This increases the probability that a neutron will escape the core, giving a negative reactivity feedback.

All analyses performed using SSC assumed that the fuel is in contact with the HT9 clad. This is the most common state for the equilibrium core since only 25% of the core will be reloaded at each refueling, and the fuel is in an unlocked state, i.e., below 2 a/o burnup, only briefly. Axial expansion is dominated by the clad after lockup since metal fuel is weak (i.e., small Young's Modulus). The fuel elongations in SSC calculations were calculated by using an average strain, weighted with Young's modulus:

$$\epsilon = \frac{\epsilon_f Y_f A_f + \epsilon_c Y_c A_c}{Y_f A_f + Y_c A_c}$$

where

ϵ = strain ($\Delta\ell/\ell$)
Y = Young's Modulus
A = Nominal cross sectional area
c = clad
f = fuel

The PRISM axial fuel expansion feedback evaluation was performed using an equation similar to Eq. (1). The reactivity worth was determined from the difference between the initial fuel length and the elongated length at any given time.

5.2.3 Sodium Density Feedback

Thermal expansion of the sodium is the only significant positive reactivity feedback, except for the long term withdrawal of the control rod drive line with vessel heatup. The thermal expansion results in fewer sodium atoms within and surrounding the core. The dominant effect is the reduction of the collisions between neutrons and sodium atoms, which hardens the neutron energy spectrum and yields a net positive reactivity feedback effect from the increased neutron importance.

The feedback formulation was of the same form as Equation (1), with the reference density at the refueling temperature. Each node was given equal weight within the given category (i.e., driver, internal blanket, and radial blanket).

5.2.4 Control Rod Drive Line and Vessel Thermal Expansion

The magnitude of this feedback is dependent upon the initial position of the control rods on the control rod worth curve. The control rod drive lines, which are in the upper internal structure, expand when they are heated, inserting

the control rods further into the reactor, adding negative reactivity.

The thermal expansion of the reactor vessel ultimately limits the amount of negative reactivity inserted by the control rod drive line. The reactor vessel is cantilevered from the top, and expands down and slowly withdraws the control rods from the core up to the control rod stop positions. The time constant for the reactor vessel is about 700s, while the control rod drive line expansion time constant is around 28s. Thus, the initial response to increased sodium outlet temperatures is a negative feedback, while the long term effect could end up being positive.

Control rod and vessel expansion are calculated in SSC using single node temperatures for the vessel and control rod drive line masses. The total elongated length is calculated by subtracting the vessel expansion from the control rod drive line expansion to determine the net control rod expansion into the core.

5.2.5 Radial Expansion

The radial dimension of the core is determined largely by assembly spacing. This spacing is determined by the grid plate below the core and by two sets of load pads above the core. When the structures heat up and expand it increases the core radius, which reduces the core average density in the radial direction. The effect increases neutron leakage and generates a negative feedback response.

In the SSC calculation, no credit was given for the thermal bowing of the assemblies. It is noted that the bowing effect may reduce the risk associated with several severe accident sequences. However, the total worth of the (limited-free) bowing carries significant uncertainties. Bowing should add negative reactivity to the system. At this time, it doesn't appear that bowing can insert any positive reactivity during any portion of the postulated accidents reviewed to date. Hence, neglecting it is a conservative assumption.

SSC tracks the radial expansion of the core from thermal expansion only. This is accomplished by tracking the structure temperatures at the above core load pads (just above the fueled area) and at the grid plate.

The coefficients supplied for radial expansion were calculated using a uniform increase over the core radius. However, the above core load pad (ACLP) responds to the core exit sodium temperature while the grid plate responds to the core inlet temperature. This causes non-uniform expansions, and the worth of each component must be weighted. From geometrical considerations, the split for PRISM is 65% from ACLP and 35% from grid plate, and this was utilized in both the BNL and GE calculations.

5.2.6 GEM Modeling

The GEM is essentially an empty assembly duct, sealed at the top, open at the bottom and connected to the high pressure in the inlet plenum of the core.

The range of operation of the GEMs tested in FFTF can be seen in Figure 5. A hexagonal cross section duct, with a wall thickness slightly greater than the standard fuel and blanket duct, forms the unit. When the pumps are at full flow, the plenum pressure (minus the static heat to the GEM level) compresses the gas in the GEM cavity to the portion of the GEMs above the core. This causes more neutrons to be scattered and deflected back into the core, as compared to when the gas is adjacent to the core. When the flow decreases, the trapped helium expands and drops the sodium level into the core region. As a result, fewer neutrons are scattered back into the core region. The effect increases as the gas expands into the core, until the gas-liquid interface drops below the core. At this point the maximum negative reactivity of 69 cents (i.e., 23 cents each) is imposed. This device offers a passive negative feedback which can protect the power-to-flow ratio during sudden loss of flow events.

In SSC, three equations are solved iteratively until they converge to give the correct sodium level in the GEMs. They are

$$Vt = V_\ell + Vg \tag{2}$$

$$Pg - \rho * h\ell = Pci \tag{3}$$

$$Pg * Vg = Mg * R * T \tag{4}$$

where

Vt	=	total GEM volume	(m**3)
V_ℓ	=	GEM sodium volume	(m**3)
Vg	=	GEM gas volume	(m**3)
Pg	=	GEM gas pressure	(Pa)
Pci	=	Core Inlet Plenum pressure	(Pa)
ρ	=	sodium density	(kg/m**3)
g	=	gravity	(m/s**2)
A	=	GEM area	(m**2)
h_ℓ	=	sodium level in GEM	(m)
Mg	=	Mass of Helium in GEM	(kg)
R	=	helium gas constant	(-)
T	=	GEM gas temperature	(K)

The gas temperature closely follows the GEM shell temperature which is determined by tracking the heat transfer between the neighboring assemblies and the GEM

$$Cp * Mg * dT/dt = Q \tag{5}$$

where Cp = GEM helium specific heat (J/kg*K)
Q = heat from conduction from surrounding fuel assemblies (watts),
t = time (s)

These equations are solved at each time step to determine the sodium level in the core. The worth of the GEMs when the level is equal to, or greater than, the top of the core is zero. When the level reaches bottom of the core, the GEMs are worth -69 cents. Intermediate levels are interpolated.

6. ANALYSIS OF UNSCRAMMED EVENTS

The transient response of the PRISM module to various unscrammed events was evaluated using SSC, and complemented using MINET calculations when necessary. SSC has been benchmarked against both ARIES (G.E.) and SASSYS (ANL) (Ref. 6) over the years, and has consistently generated similar results for similar events. The calculations contained in this section used models that were more conservative than those used by the vendor.

Three unscrammed (beyond design base accidents) events are covered in this section. They are the unscrammed loss of heat sink (ULOHS), loss of flow (ULOF), and the transient overpower (UTOP) event. This set of transients is not all inclusive, but it does demonstrate the passive shutdown response of the current PRISM design.

6.1 Unscrammed ULOHS

This event is initiated by a sudden stoppage of the intermediate loop flow. Physically, this would be equivalent to the intermediate loop sodium being dumped into the system dump tank during a sodium-water reaction event. All heat generated after that event is retained in the reactor module. The reactor scram system is also assumed to fail, while the rest of the system continues to function. The initial operating conditions for PRISM, and the corresponding initial conditions from SSC are shown in Table 2.

Table 2
Table of Initial and Key Operating Parameters

Description	PRISM	SSC
Power (MW_t)	471	471
Cover Gas (kPa)	99.3	99.3
Primary Flow (kg/s)	2513	2507
Primary Sodium Inlet (K)	610.9	610.9
Primary Sodium Outlet (K)	758.1	758.0
Core Height (m)	1.342	1.3462
Peak Fuel Pin/Average Fuel Pin	1.31	1.31
Fuel Pin OD (m)	.00668	.00668
Driver Fuel Pins/Assembly	331	331
Intermediate Sodium Flow (kg/s)	2293	2275
Intermediate Sodium IHX Inlet (K)	555.4	557.0
Intermediate Sodium IHX Outlet (K)	716.5	720.0

The system remains at rated power for many seconds. The slow increase of core inlet sodium temperature, due to the large thermal mass in the cold pool, is shown in Figure 6. The figure also indicates that the power begins to transition downward once the core inlet temperatures increase significantly. The core outlet temperature does not pass through the same temperature increment as the inlet because the core power is decreasing.

The increase in the core inlet temperature had a dramatic effect on the neutronic feedbacks as shown in Figures 7 and 8. The total reactivity remained constant (at zero) until the higher temperature sodium entered the core. A negative feedback then resulted from the thermal expansion of the fuel (axial), the core radius, and control rod drive line. Those effects were only slightly countered by the positive sodium density effect. It should be noted that the control rod drive line's negative reactivity worth was reduced after 200 seconds by the thermal expansion of the reactor vessel, which pulls the control rods from the core (Figure 8). The net effect is that the increase in core temperature generated a negative reactivity response, which reduced the power to decay heat levels by 500s.

A representative temperature profile for a peak node in the hot channel is shown in Figure 9. The temperature decrease after 75s is representative of all the mid-core fuel temperatures. Some of the fuel centerline temperatures below the core mid-line increased because of the higher inlet sodium temperatures, but these locations do not contain the limiting fuel temperatures. The ability of the reactor to transition to a lower power level removes the concern of fuel failure for this event. Figure 10 shows the margin to sodium saturation is about 560K.

Thus, the ULOHS event does not present a significant challenge to the PRISM passive shutdown response. The peak fuel temperatures decrease; thus there is no concern for fuel damage for the calculated event. The only issue might be the length of time this transient is allowed to continue and the impact on service limits. A remaining safety issue is the tendency of the vessel to expand and pull the control rods out of the core (to the rod stop position) which reduces the negative worth and can even insert positive reactivity. However, the ultimate shutdown system could be activated to establish shutdown, and would preclude prolonged unscrammed events.

6.2 ULOF Events

The loss of flow event is assumed initiated by a trip and coast down of the EM pumps from full power (Table 2). It is further assumed that the secondary loop continues to operate and the scram signal fails to insert the rods. This event was the most challenging for the previous design, which did not include GEMs. Since GEM reliability is still an issue, we analyzed this event for a ULOF with and without GEMs.

6.2.1 ULOF with GEMs

The trip and coast down of the pumps results in a power reduction almost immediately (Figure 11). Figure 12 shows that the core outlet temperature peaks

at about 50K above operational and drops to below 700K by 300s. Power deceases and reduces the peak fuel temperature (Figure 13). Consequently, no fuel damage would be expected.

The various reactivity feedbacks are shown in Figures 14 through 16. The total reactivity was predicted to quickly drop to -40¢, then slowly back off to -15¢ by 600s. The grid plate and ACLP in Figure 14 are the components of the radial expansion term on Figure 15. The grid plate is in contact with the inlet sodium, which experiences little change in temperature, while the ACLP above the core sees a reduction in core exit temperatures. This causes a contraction and insertion of positive reactivity. The core cool down causes a contraction from the fuel (axial expansion), sodium density (this is a negative effect), and the control drive line. These effects, except for the sodium density, are all positive reactivity feedbacks. The dominant negative feedback is the GEMs, which reduces the power in proportion to the core inlet plenum pressure and overrides the positive reactivity feedback from the thermal contractions. Thus, the overwhelming negative feedback from the GEMs causes the core power to decrease to decay heat levels by 500s. The fact here is that the reactor power level is reduced by the GEMs, rather than a balance established between the thermal expansion (or contraction) feedbacks of the core. Consequently, the GEMs function more like passive control rods, with the reactivity worth dependent on the core inlet pressure for this event. Finally, Figure 17 shows the margin to sodium boiling to be approximately 300K with the GEMs.

6.2.2 ULOF Without GEMs

This event was analyzed identically to the ULOF with GEMs, except for the removal of the GEMs from the modeling. From Figures 11 and 12, it can be seen that the power and core outlet temperature are higher than the previous case. The power level drops to about 10% of the initial power level by 600s, which results in the core outlet temperature being about 100K above the case with GEMs.

The neutronic feedback behavior for the case without GEMs is quite different, as shown in Figures 18 through 20. Without the GEMs, there isn't a large dominant negative feedback. Actually, the increase in temperature in this event generates the transition to a lower power by establishing a new reactivity balance between the thermally activated feedbacks. Heating up the sodium flowing in the core generates a negative feedback from radial expansion (i.e., ACLP), axial expansion, and control rod drive line thermal expansion. The Doppler term is initially negative since the core average temperature of the fuel increases, but as the power declines, the average fuel temperature decreases and turns positive. The increase in the sodium temperatures contributes a positive response. However, the feedbacks all combine to produce a net negative feedback which reduces the core power to 10% by 600s.

The difference between the two cases with and without GEMs can be judged in terms of the peak fuel and sodium temperature. As shown in Figure 21, the peak fuel temperature was predicted to be 1150K which is higher than before, but still lower than the solidus temperature of the fuel, which is 1249K. As shown

in Figure 17, the peak sodium temperature in the core came within 160K of the saturation temperature, which remains a significant margin.

6.2.3 ULOF Conclusion

The SSC predictions indicate PRISM would be able to withstand the ULOF events with and without the GEMs. When available, the GEMs dominate the neutronic feedbacks and bring the power down to decay heat levels within 500s, with a margin to sodium boiling of 300K. The fuel temperatures decrease demonstrates that fuel damage is not a significant risk for this event. For the case without the GEMs, SSC predicted that the thermal expansion feedbacks would be activated and combine to reduce power to 10% rated by 600s. The fuel temperatures for the case without GEMs do not indicate significant damage, but the margin to sodium boiling is reduced to 160K. Without the GEMs, however, there could be a small amount of cladding wastage during this event.

6.3 UTOP

An unprotected transient over power (UTOP) accident results when positive reactivity is inadvertently inserted into the core, leading to increased reactor power. The scram signal is assumed to fail to insert the rods. The limiting case is the accidental withdrawal of all of the control rods. This event is bounded by the excess amount of reactivity in the core. In an oxide core, the temperature and power defect, along with the built in excess reactivity for the burnup swing, can amount to several dollars. This makes the event very severe. In the metal fuel core of PRISM, a small temperature and power defect (~$1.2) and negligible burnup swing (~$0.04), and the excess reactivity to account for a fuel axial growth with exposure, are the only excess reactivities built into the system. The amount of potential reactivity available for the insertion is reduced further by adding control rod stops, which reduce the available reactivity by limiting withdrawal distance. GE's current objective is for the rod stops to prevent the net rod insertion worth available for withdrawal from exceeding 40¢, which includes a 10¢ uncertainty allowance. The reference PRISM UTOP rate is 2¢/s (since it is the maximum control rod withdrawal speed to a total of 40¢).

6.3.1 Component Migration and the UTOP Event

Based on experimental data from EBR-II, it is clear that annular zones develop in the ternary metal fuel pins during burnup. Component migration changes the local thermal conductivity, solidus and liquidus temperatures, which impact the peak fuel temperatures and the margin to fuel melting. In addition, any plutonium migration could redistribute the power within the pin. The SSC calculations here used the most conservative estimation of the thermal conductivity, which included the effect of plutonium and zirconium migration, as well as a redistribution of power in the pellet. These calculations will be re-evaluated and revised as new ternary fuel data becomes available.

Starting from normal operating conditions (Table 2), a reactivity insertion of 2¢/s was continued for 20s, for a total of 40¢. It was further assumed that the scram system failed to insert the control rods, but that the rest of the

system (i.e., IHX, EM Pumps) continued to function. The power increase for this event would be limited in an oxide core by the Doppler effect. However, in PRISM's metal fuel core, the thermal expansion (negative) feedbacks must supplement the (small) Doppler feedback to terminate the power excursion.

The power is predicted to reach 1.8 times the rated level (Figure 19), and then falls back to about 1.2 times the rated power level. The core outlet peaks at about 880K, and drops to 840K after the new power level has been stabilized by the reactivity feedbacks.

The reactivity feedbacks of the system are shown in Figures 23 through 25. The total reactivity increases during the control rod withdrawal process. The components of the radial expansion term, shown in Figure 23, indicate that the ACLPs respond quickly to the increase in exit sodium temperature, while the grid plate reactivity is delayed until hotter sodium enters the core. The reactivity figures indicate that the increased temperatures resulting from the power increase activates the thermal expansion (negative) reactivities. This reverses the power increase and gradually reduces the power to 1.2 times the rated power level. The only positive feedback in the system was due to the decreased sodium density, which contributed less than 10¢ during the event.

The peak fuel temperatures at the hottest location can be seen in Figure 26. The fuel temperatures reaches 1400K, which is far above the solidus temperature for nominal fuel (i.e., ~1275K). Further, if we consider the migration of the zirconium and uranium components, the local solidus temperature could be as low as 1200K. Both the ARIES (GE) and SSC (BNL) calculations predicted some melting. The GE analysis predicted a small fraction of melting for a few seconds while the SSC results, reflecting reduced thermal conductivity due to component migration, predicted a significant fraction of the peak pin to melt. The degree and possible acceptability of local fuel melting during a postulated 40¢ UTOP is an open issue. Certainly G.E. has some options for reducing the size of potential UTOP initiators, e.g., by moving the control rod stops more frequently. However, the performance of the ternary metal fuel is not fully understood at this time, and the fuel developers at ANL are hopeful that further data will support their position regarding the acceptability of the 40¢ UTOP. The margin to sodium boiling (Figure 27) was predicted to be about 340K.

7.0 SUMMARY

The revised PRISM design has been evaluated using SSC for an unscrammed loss of heat sink (ULOHS), an unscrammed loss of flow (ULOF) with and without the Gas Expansion Modules (GEMs) functioning, and a 40¢ unscrammed transient overpower (UTOP) event. The feedback effects for U-27Pu-10Zr fuel were modeled. The ULOHS accident was predicted to be a benign event for the design, with the reactor power transitioning down to a decay heat level within 500s. The power during ULOF events, with the GEMs functioning, decreases to decay heat levels without causing fuel damage and leaving a 300K margin to sodium saturation. The case without the GEMs had a 160K margin to sodium saturation and higher fuel temperatures. The clad was predicted to quickly pass through the eutectic phase

(between fuel and clad), which would waste some clad. The 40¢ UTOP was predicted to raise the power to 1.8 times rated power initially, with the power later decreasing to 1.2 times rated power. SSC predicted some localized fuel melting for the event, but the significance of this localized damage has not yet been determined. If necessary, the vendor has options to reduce the maximum reactivity insertion below 40¢.

REFERENCES

Ref. 1 R. R. LANDRY, T. L. KING, and J. N. WILSON, Draft Preapplication Safety Evaluated Report for Power Reactor Inherently Safe Module Liquid Metal Reactor, Nuclear Regulatory Commission Report, NUREG-1368, September 1989.

Ref. 2 G. J. VAN TUYLE, G. C. SLOVIK, B. C. CHAN, R. J. KENNETT, H. S. CHENG, and P. G. KROEGER, Summary of Advanced LMR Evaluations - PRISM and SAFR, Brookhaven National Laboratory Report, NUREG/CR-5364, BNL-NUREG-52197, October 1989.

Ref. 3 G. L. GYOREY, D. R. PEDERSON, and S. ROSEN, Safety Aspects of the U.S. Advanced Liquid Metal Cooled Reactor Program, Proceedings of the 1990 International Fast Reactor Safety Meeting, Snowbird, Utah, August 12-16, 1990.

Ref. 4 J. G. GUPPY, et al., Super System Code (SSC, Rev. 0) An Advanced Thermohydraulic Simulation Code for Transients in LMRBRs, NUREG/CR-3169, BNL-NUREG-51659, April 1983.

Ref. 5 G. J. VAN TUYLE, T. C. NEPSEE, and J. G. GUPPY, "MINET Code Documentation", NUREG/CR-3668, BNL-NUREG-51742, Brookhaven National Laboratory, February 1984.

Ref. 6 F. E. DUNNE, et al, "The SASSYS-1 LMFBR Systems Analysis Code", ANL/RAS 84-14, June 1984.

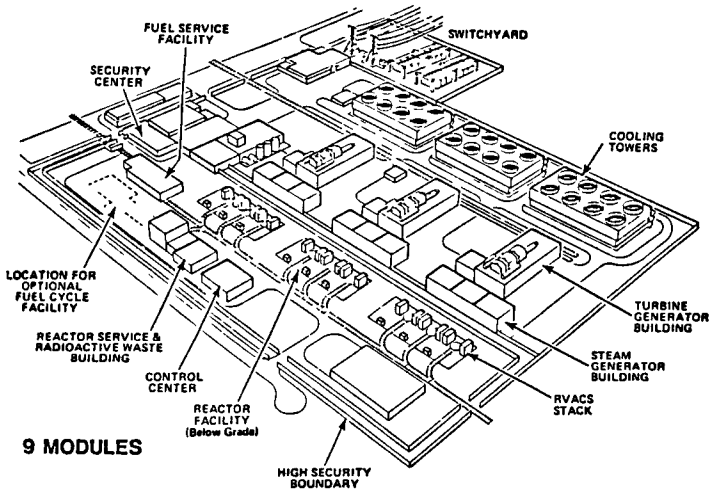

Figure 1. The 1395 MWe ALMR Power Plant With 3 Power Blocks

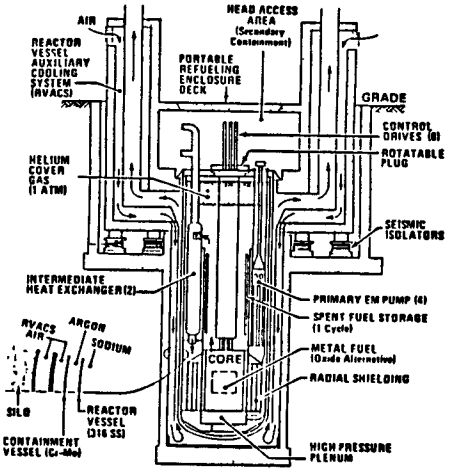

Figure 2. ALMR Reactor Module

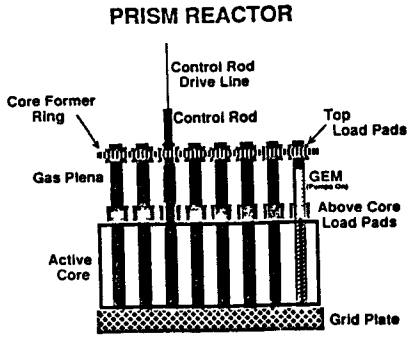

Figure 3. PRISM Core

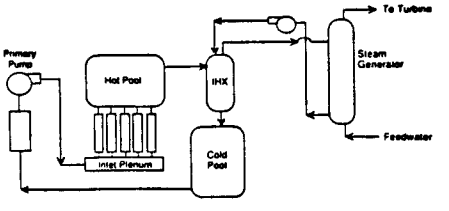

Figure 4. SSC Representation of LMR Systems

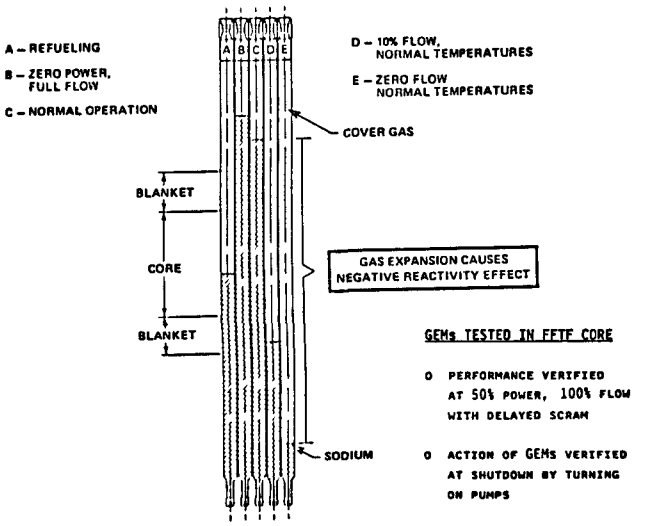

Figure 5. Operation of the Gas Expansion Module (GEM) Tested in FFTF (Which has a Similar Behavior in PRISM)

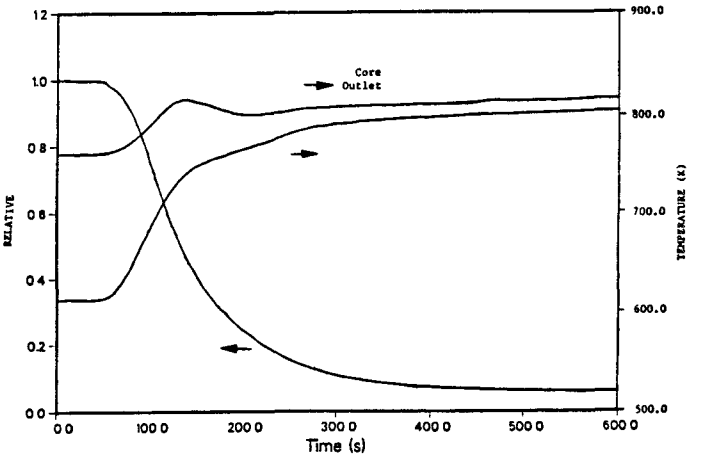

Figure 6. Predicted Core Outlet and Inlet Temperature Along with the Relative Power from SSC for ULOHS

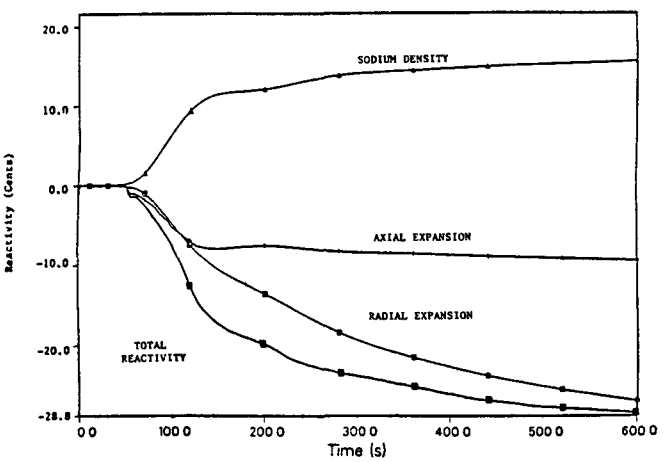

Figure 7. Predicted Neutronic Feedback from SSC for a ULOHS

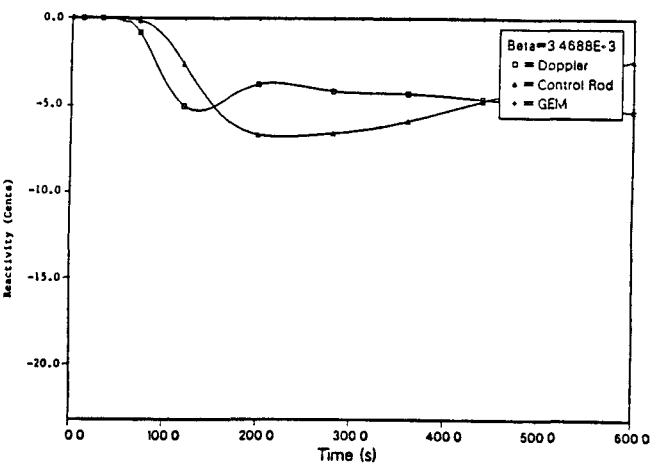

Figure 8. Predicted Doppler, Control Rod Expansion, and GEM Reactivity Feedback from SSC for a ULOHS

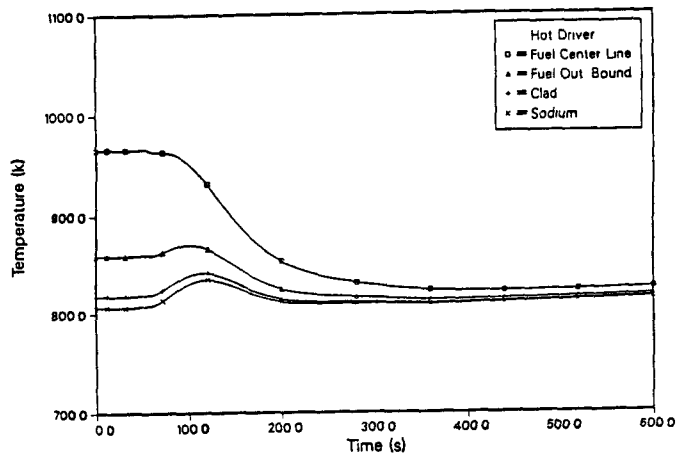

Figure 9. Predicted Fuel Temperature Distribution from SSC for the TOP Node (i.e., 1.346 m - 1.122 m) for a ULOHS

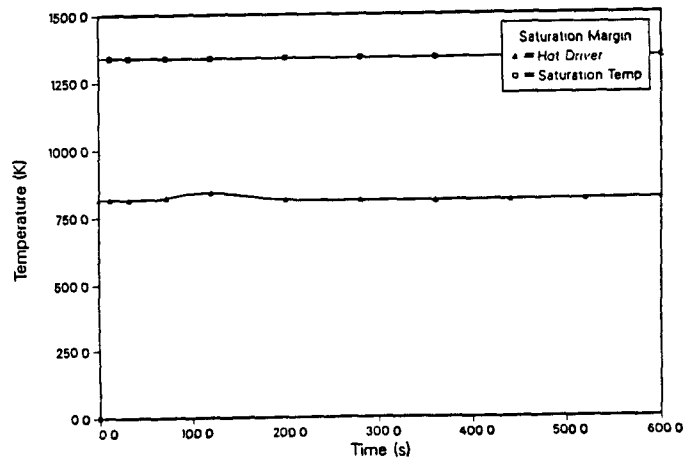

Figure 10. Predicted Margin to sodium Saturation from SSC for a ULOHS

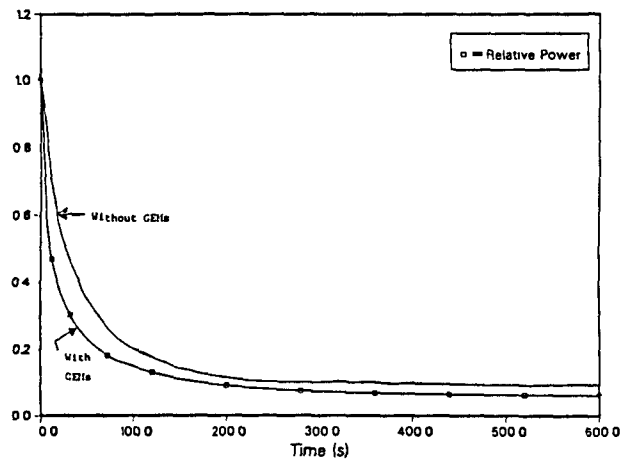

Figure 11. Predicted Relative Power from SSC for a ULOF With and Without GEMs

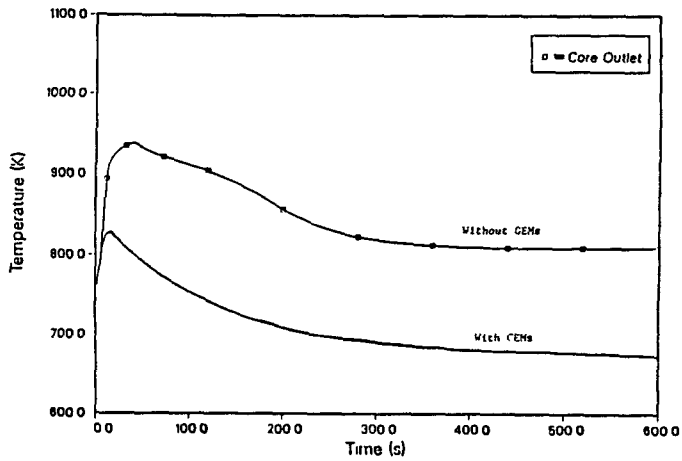

Figure 12. Average Core Outlet Temperature from SSC for a ULOF With and Without GEMS

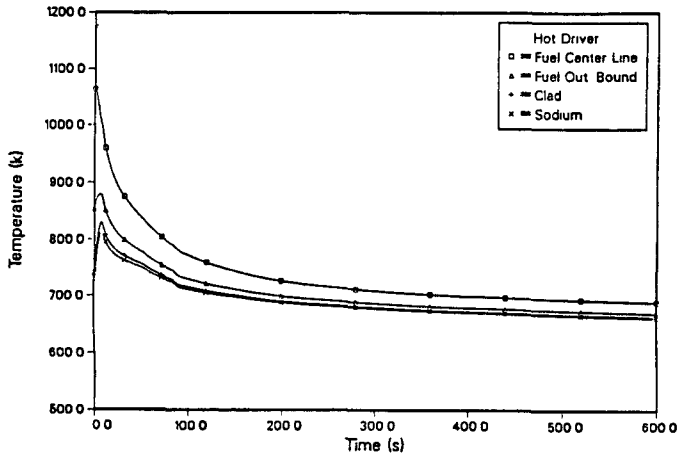

Figure 13. Predicted Fuel Temperature Distribution from SSC for the Third Node from the Top (i.e., 0.897 m - 0.673 m) for a ULOF with GEMs

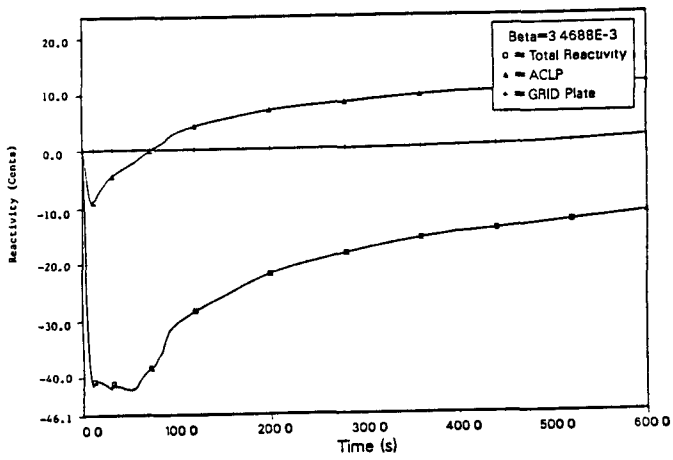

Figure 14. Predicted Total, ACLP, and GRID Plate Reactivity Feedback from SSC for a ULOF with GEMs

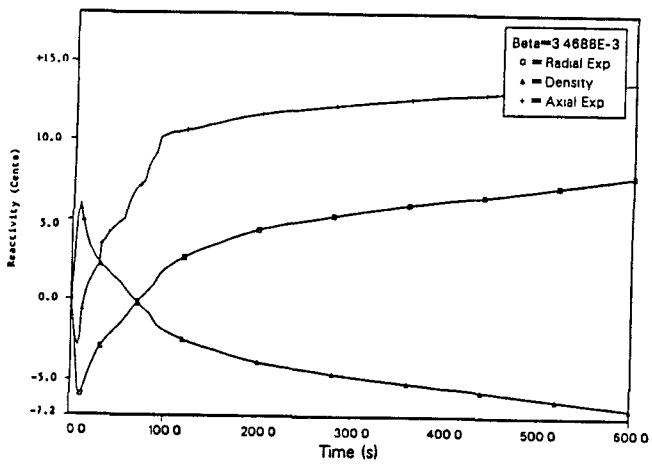

Figure 15. Predicted Radial Expansion, Sodium Density, and Axial Expansion Reactivity Feedback from SSC for a ULOF with GEMs

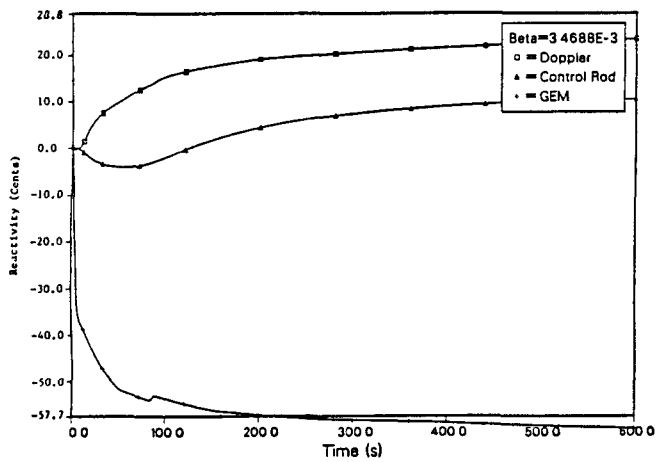

Figure 16. Predicted Doppler, Control Rod Expansion, and GEM Reactivity Feedback from SSC for a ULOF with GEMs

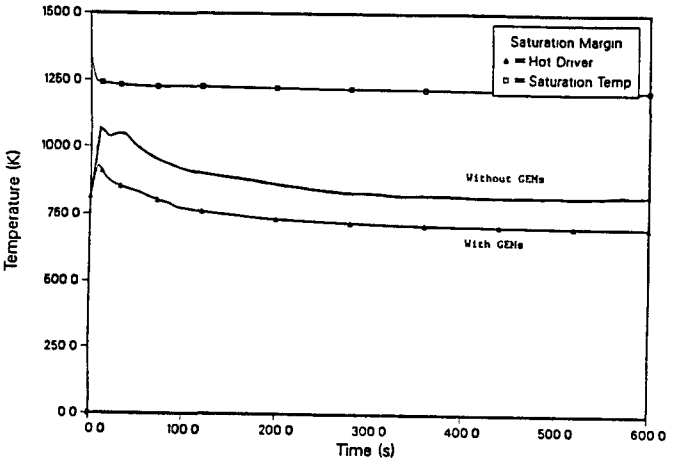

Figure 17. Predicted Margin to Sodium Saturation from SSC for a ULOF With and Without GEMs

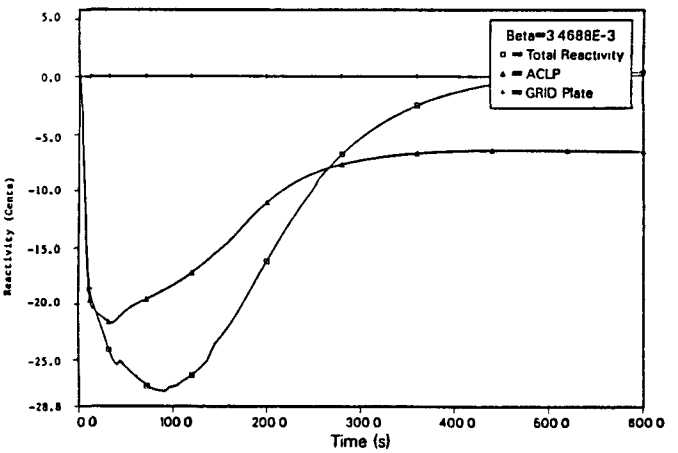

Figure 18. Predicted Total, ACLP, and GRID Plate Reactivity Feedback from SSC for a ULOF Without GEMS

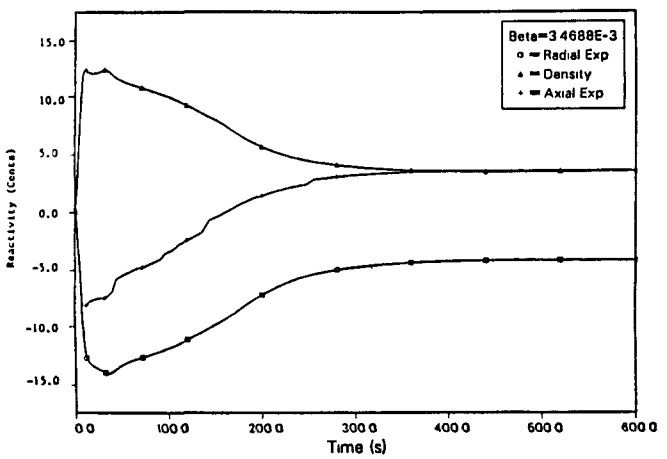

Figure 19. Predicted Radial expansion, Sodium Density, and Axial Expansion Reactivity Feedback from SSC for a ULOF Without GEMs

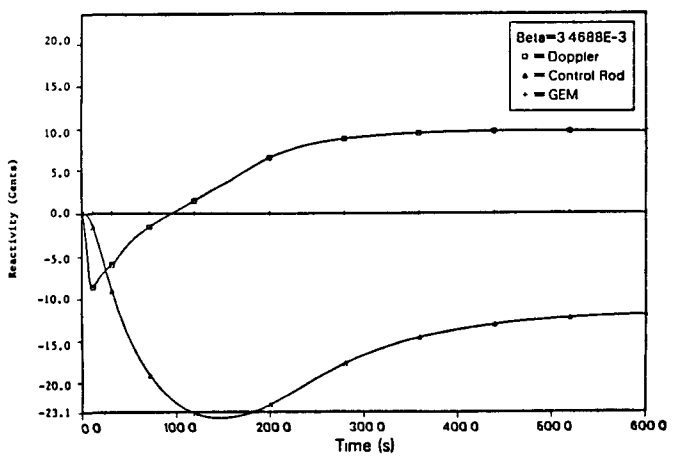

Figure 20. Predicted Doppler, Control Rod Drive Line Expansion, and GEM Reactivity Feedback from SSC for a ULOF Without GEMs

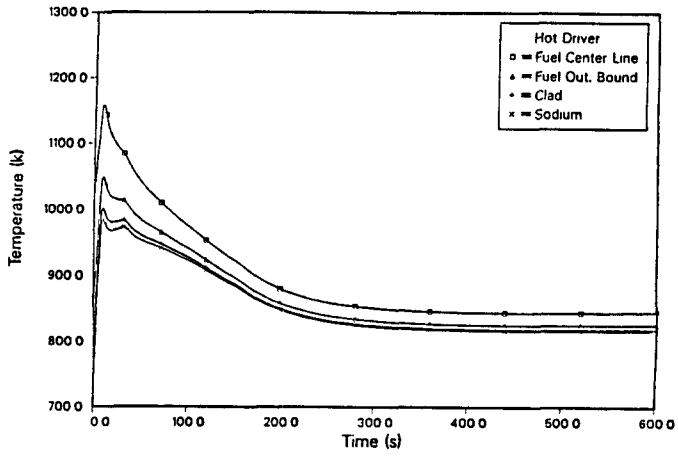

Figure 21. Predicted Fuel Temperature Distribution from SSC for the Second Node from the TOP (i.e., 1.122 m - 0.897 m) for a ULOF Without GEMs

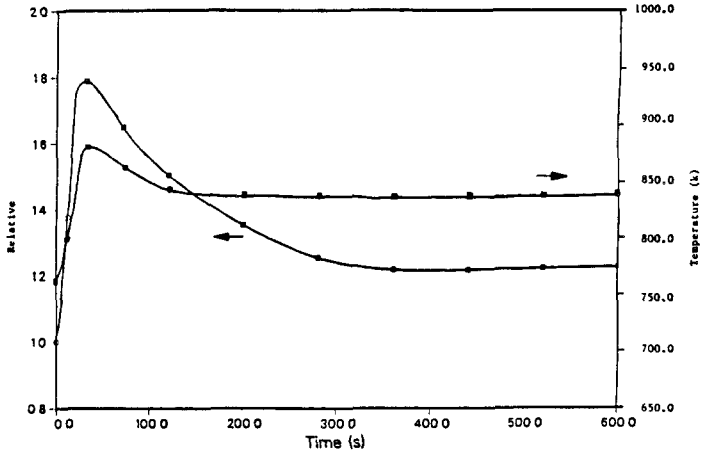

Figure 22. Relative Core Power and Average Core Outlet Temperature Predicted by SSC for PRISM During a 40 Cent UTOP

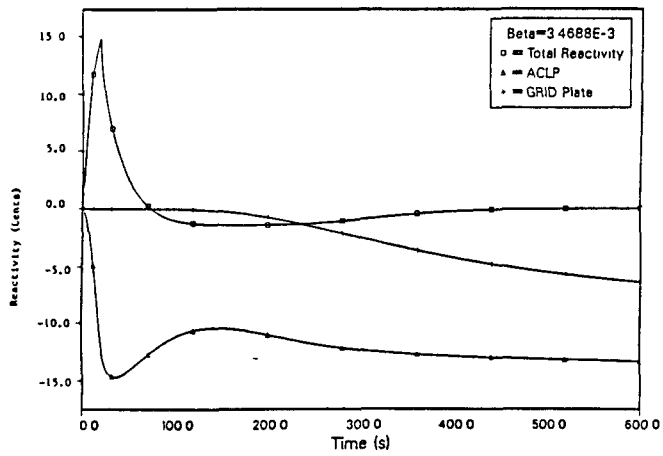

Figure 23. Predicted Total, Above Core Load Pad (ACLP) and Core Support Grid Plate Reactivity Feedback from SSC for a 40 Cent UTOP

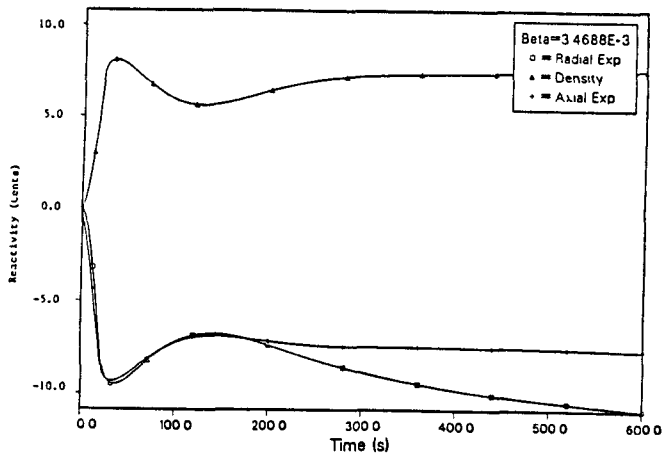

Figure 24. Predicted Radial Expansion, Sodium Density (Density), and Axial Expansion Reactivity Feedback from SSC for a 40 Cent UTOP

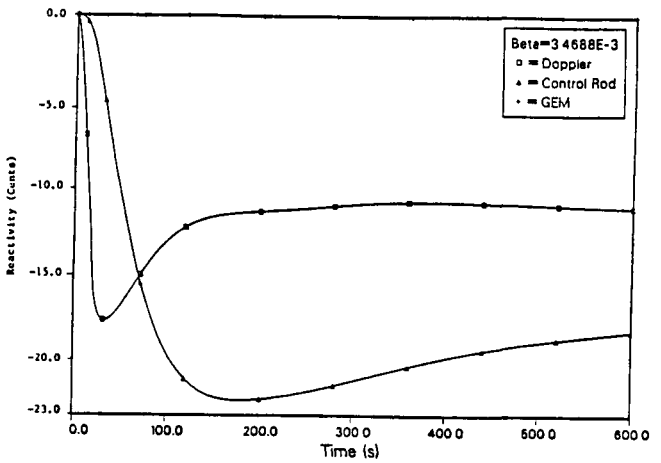

Figure 25. Predicted Doppler, Control Rod Expansion, and Gas Expansion Module (GEM) Reactivity Feedback from SSC for a 40 Cent UTOP

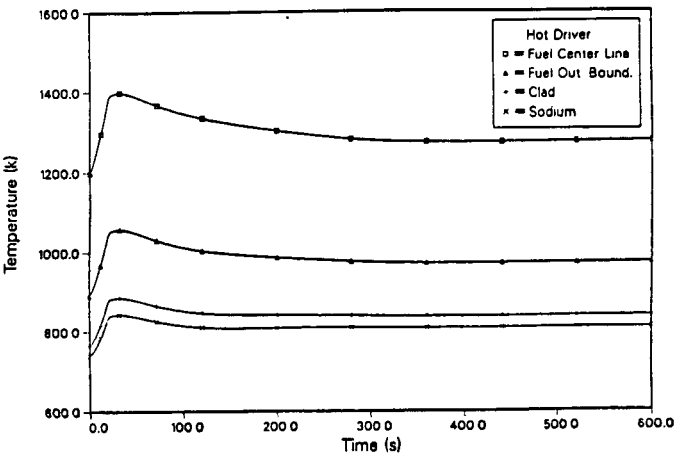

Figure 26. Predicted Fuel Temperature Distribution from SSC for the Third Node from the Top (i.e., 0.897 m - .673 m) During a 40 Cent UTOP

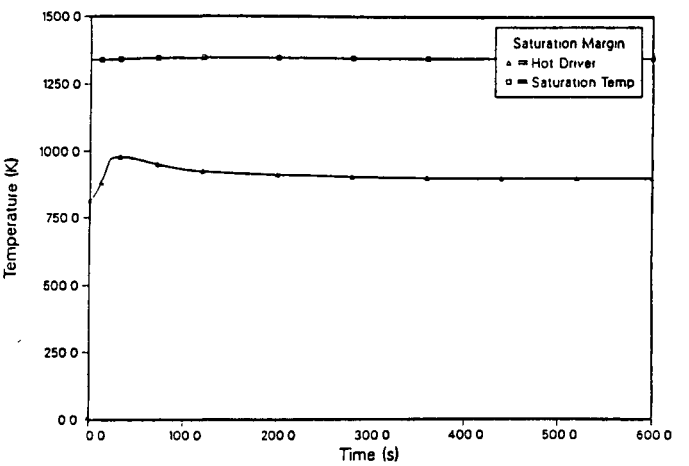

Figure 27. Predicted Sodium Saturation Margin from SSC for the 40 Cent UTOP